Designing Radiation Shielding for a Deuterium-Deuterium Neutron Generator

A Major Qualifying Project

Submitted to the Faculty of

Worcester Polytechnic Institute

In partial fulfillment of the requirements for the

Degree in Bachelor of Science in Physics

By

Hope Clairmont

Date: 5/13/2020

Project Advisor

Professor David Medich

Abstract

The effectiveness of several different materials to attenuate various kinds of radioactive particles produced was examined using the WPI physics department's deuterium-deuterium neutron generator. Radioactive materials have many practical applications, from radiation therapy in medicine to nuclear power, but they can be dangerous to nearby humans and their surroundings. As such, shielding materials are required on any device that uses or produces radioactive materials. I conducted a series of experiments to determine the optimal shielding design for our generator.

Acknowledgements

I would like to thank Professor Medich for giving me the opportunity to work on this project, as well as all of his invaluable advice and support every step of the way.

I would like to thank Justine Dupere for all of her help in the lab, for letting me bounce ideas off of her, and for helping me carry so many heavy bricks.

Finally, I would like to thank my family and friends for supporting me through this entire process, even as the world turned itself upside down.

Table of Contents

1. Introduction

Radiation and radioactive materials have practical applications in a myriad of fields. Neutrons, in particular, are interesting because they are a fundamental particle in the atomic nucleus and are chargeless. Neutrons are used in research to determine the elemental makeup of substances, examine construction materials for cracks and other microscopic defects, and have even been investigated for use as a radiotherapy source (Lou, 2003, p. 11). Despite their usefulness, until recently very few laboratories had access to neutron sources. This is because the only way to create a beam of neutrons was to use either difficult to obtain radioactive materials such as 252 Cf, 239 PuBe, or 241AmBe; a fission source, such as a research reactor; or a spallation neutron source, which accelerates protons into a heavy atomic nucleus to excite it and cause it to release a neutron (Lou, 2003, p. 11). However, these methods present significant drawbacks, chief among which are a high cost, a wide and often uncontrollable flux of neutron energies, and an elevated risk in event of an accident (Lou, 2003, p. 9-14).

The advent of compact deuterium-deuterium neutron generators has changed this reality. Neutron generators have a relatively low price compared to other neutron sources and have the ability to create neutrons of a specific desired energy. These advancements led to the widespread adoption over the past decade and have enabled smaller laboratories that otherwise could not afford to conduct experiments with neutron sources to enter the field.

The WPI neutron generator comes with some built-in shielding system. This system consists of an innermost layer of the hydrogenous plastic polyethylene several centimeters in width, followed by a layer of borated polyethylene of roughly the same width, with an external layer of lead less than a centimeter thick (Adelphi Technology, 2016, p. 5). Yet, even with this shielding system, the generator must be placed in a thick shielded room (with walls of ~3-4” thick concrete). The goal of this project is to determine the optimal shielding material and geometry for the neutrons emitted from our D-D Neutron Generator.

Previous experiments have been conducted with deuterium-tritium neutron generators, which operate on very similar principles to deuterium-deuterium generators (Chichester & Blackburn, 2007, p. 845). These studies found that materials with lower atomic numbers such as polyethylene or concrete are by far the most effective for shielding because they are capable of stopping both neutrons and the secondary photons created by them upon their interaction (Chichester & Blackburn, 2007, p. 845). Polyethylene was found to be most effective, with borated polyethylene and concrete following close behind. Materials with higher atomic numbers such as lead fared poorly, because the 14.1 MeV neutrons produced by the generator may excite these denser materials, producing more neutrons, while the same effect does not occur in hydrogenous materials.

This first takeaway is likely to hold true for WPI’s neutron generator, as the underlying physics of their interactions with the neutrons produced by our generator are the same. As such, these materials were investigated for their usefulness in shielding in this experiment. However, since the neutrons produced by WPI’s deuterium-deuterium generator have much lower energies than those produced by a deuterium-tritium generator, the potential reaction pathway that makes these materials poorer shielding is less of a concern. As such, one such material, lead, was also investigated by this experiment. My hypothesis is that the ideal shielding system for the generator will be similar to the one it came with, consisting of an interior layer of a low atomic number material to absorb neutrons, with a thin exterior layer of a high atomic number material to absorb photons.

2. Background to the project

2.1 Kinds of radiation produced by generator

There are three main kinds of radiation produced by the deuterium-deuterium neutron generator that a shielding system must be able to attenuate. The first are the thermal neutrons which the generator is designed to produce. These are neutrons with kinetic energies similar to those of air molecules at room temperature, approximately 0.025 eV (Editors of Encyclopaedia Britannica, 2018). The second are fast neutrons, neutrons with energies sufficient to cause ionization when they interact with an atom. These fast neutrons are scattered off a polyethylene moderator to convert them into thermal neutrons, and almost uniformly have an energy of 2.5 MeV (Adelphi Technology, 2016, p. 6). (This process is discussed further in section 2.2.)

These are the only two kinds of radiation produced directly by the generator, but any shielding system must also account for bremsstrahlung and absorption gamma-rays. Bremsstrahlung refers to photons that are produced when an electron loses energy due to interactions with electromagnetic fields (Kunashenko, 2011, p. 2). While high-energy electrons are not produced directly by the generator, they can be produced by the interaction of thermal or fast neutrons with shielding material. Absorption gamma rays are similarly produced when a neutron is absorbed by shielding material, such as boron, which then creates an energetically unstable new isotope of boron that becomes more stable by emitting a gamma ray from its nucleus.

2.2 Operation of Generator

The deuterium-deuterium neutron generator is designed to produce a steady beam of thermal neutrons. To create them, deuterium gas is bombarded by microwaves, ionizing the deuterium to produce a positively charged deuterium plasma. Then, a titanium target within the generator is negatively charged to high potential, causing the deuterium ions to accelerate towards it at high velocities. The first ions to strike the titanium will bond with nearby atoms to the compound titanium hydrate, which fixes the deuterium atoms in place. When another deuterium ion strikes the captured deuterium atom, fusion will occur, producing a helium atom and a “fast” neutron with an energy of 2.5 MeV. These neutrons then enter a moderator, which lowers their energy to 0.0025 eV; the thermal neutrons are then allowed to leave the moderator through a pinhole opening, creating a beam of thermal neutrons (Adelphi Technology, 2016, p. 5).

The neutron generator comes with its own shielding, which consists of polyethylene, borated polyethylene, and lead (the shielding properties of these materials are discussed section 3.2). However, this shielding is designed to be easily removed from the sides of the generator. When removed, the fast neutrons produced by the fusion of deuterium can escape out of the side of the generator (Adelphi Technology, 2016, p. 7).

2.3 Shielding Theory

The materials that will be most effective for shielding are the ones with the highest stopping power. Stopping power is the average rate of linear energy loss per unit length that a specific kind of radiation, with a specific energy, loses as it travels through a specific material. The equation for stopping power is:

$$S = \frac{-dE}{dx}$$

Where *S* is the stopping power, E the current energy of the particle, and x the distance it has traveled through the material. When this differential equation is solved, it yields the following equation for the energy the particle will have after travelling a given distance x through the material:

$$E(x) = E_0 e^{-(\mu/\rho)x}$$

Here, E_0 is the original energy of the particle. This equation shows that the energy a particle loses as it travels through is an exponential function of the distance traveled, dependent only on its initial energy and the constant μ/ρ, known as the mass attenuation coefficient. This constant is different for each material and kind of radiation, as well as for particles with different energies. This means the mass attenuation coefficient for fast neutrons in a given material will not be the same as that for thermal neutrons, nor that for x-rays or gamma rays.

Therefore, in order to determine the materials that are most effective at shielding against these three kinds of radiation, we must find that material's mass attenuation coefficient for each of these particles.

3. Methods and Materials

3.1 Initial experimental design

To determine the effectiveness of various materials at shielding against both fast neutrons, thermal neutrons, and gamma and x-rays, a method was needed to measure the absorbed dose due to each individual form of radiation. As such, two different measuring devices were used. An ion chamber was used to measure the absorbed dose due to x-rays and gamma-rays. Meanwhile, a device known as a Remball was used to measure the absorbed dose due to neutrons.

Since the Remball was incapable of distinguishing between the component of the absorbed dose due to fast neutrons and the component due to thermal neutrons, another method of distinguishing the two was needed. To do so, measurements were taken at two locations. To measure the effectiveness at stopping thermal neutrons, measurements were taken in front of the generator, where the normal shielding and moderation was kept intact, letting only thermal neutrons escape the generator. To measure the effectiveness against fast neutrons, measurements were taken at the side of the generator, from which its built-in shielding had been removed, allowing fast neutrons to escape.

In both locations, the remball was placed the same distance from the generator, on tables of the same height. (The table on which the measuring devices were placed in front of the generator, for measuring thermal neutrons, had a surface made of 2.54 cm thick borated polyethylene, while the table on which the measuring devices were placed to the side of the generator, for measuring fast neutrons, had a surface made of 1.00 cm thick aluminum. This detail will become important later.) While not strictly necessary, as the only thing being measured were the relative absorbed dose without and with shielding, this step was taken to give the results some more consistency. Since bremsstrahlung and absorption gamma rays would theoretically be produced by both fast and thermal neutrons' interactions with shielding material, measurements of the absorbed dose due to gamma and x-rays were taken with the ion chamber in both locations.

To measure the effectiveness of materials at blocking radioactive particles, sheets or blocks the material with a known width would be placed in between the generator and the Remball or ion chamber. However, the laboratory in which the neutron generator is located is very confined, with only a few feet of clearance between the generator and the walls. As such, there was a high risk of radioactive particles hitting the wall or floor, and bouncing into the ion chamber or Remball, which would create elevated levels of background radiation and reduce our experimental radiation-shielding detection limit.

To prevent this radiation from affecting the measurements, collimators were built around the spot on the table where the radiation detectors would be placed during the experiments. The collimators were made of borated concrete. This material was chosen partly because of its theoretical effectiveness at shielding against both neutrons and photons (more on this subject in section 3.2), and partly because a large number of borated concrete blocks were available for use in building a collimator in the lab. When the Remball or ion chamber were placed at their designated locations on the table, the collimator would surround their sensitive area on both sides, while the measuring device itself protected the back. This is illustrated in Figure 1. Before the generator was turned on, a 2.54 cm thick sheet of borated polyethylene was placed on top of the collimator to protect the measuring device from the top. Initially, no specially attention was given to protecting the measuring device from the bottom; this will be discussed further in the section 4.

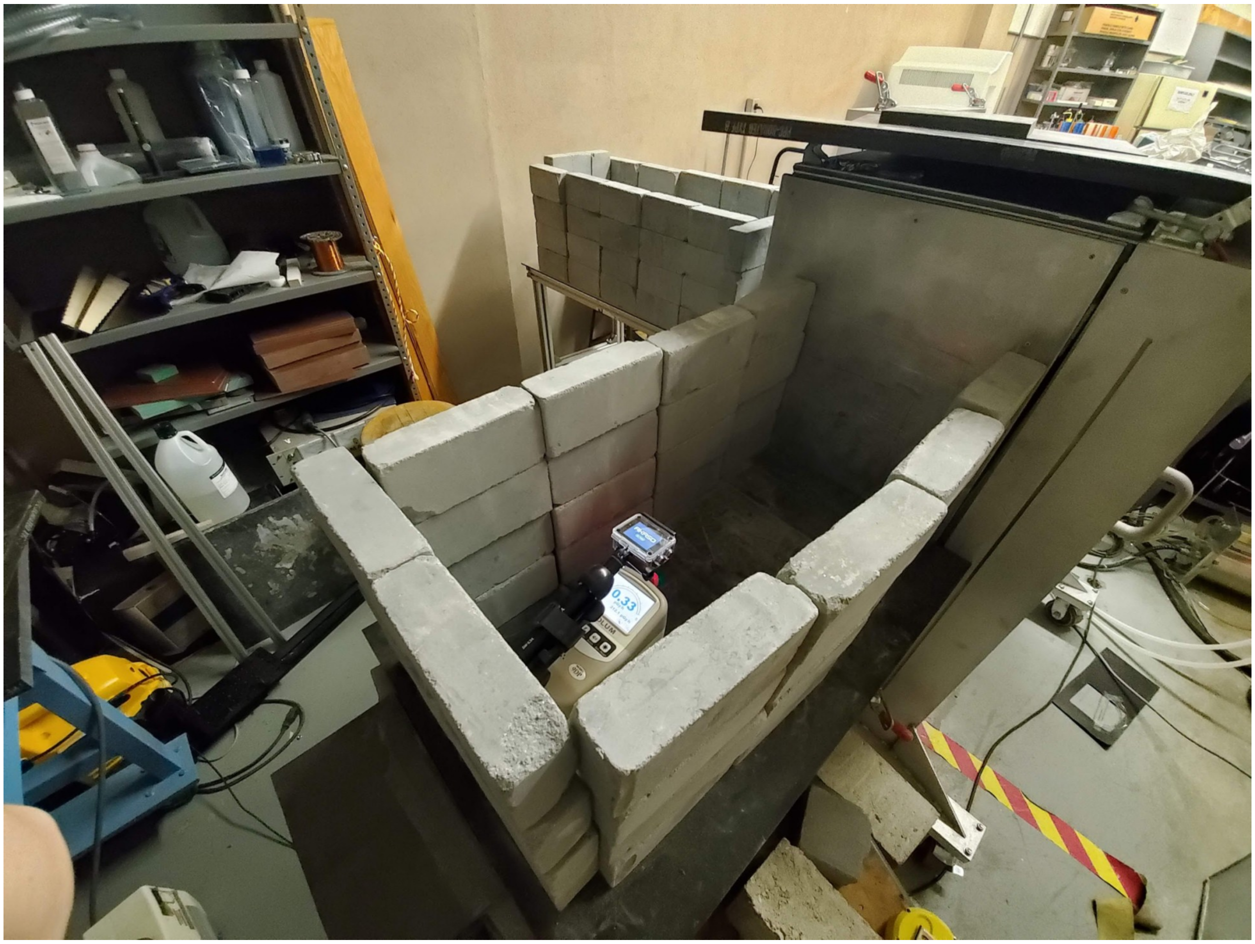

Figure 1: The collimator built in front of WPI's neutron generator, as seen from above. The ion chamber can be seen resting within the collimator. The concrete structure in the background of the picture is the side collimator; note the front collimator rests on a tabletop made of borated concrete, while the side collimator's table is aluminum.

3.2 Materials

The materials tested in these experiments were chosen based on their theoretical effectiveness at shielding various forms of radiation, as well as my ability to access them in sufficient quantities at low or no cost.

The first material tested was concrete. 3" (7.62 cm) thick cinder blocks were stacked on top of one another to create a wall blocking the mouth of the collimator. Concrete, rich in hydrogen and other light elements, should theoretically be effective at capturing neutrons both fast and thermal (Martin, 2013, p. 660). Also tested for effectiveness was borated concrete, which is a kind of concrete with significant quantities of boron added to its chemical composition. Boron has a very high absorption cross-section for neutrons, meaning it theoretically should be very effective at shielding against them (Martin, 2013, p. 660). By adding boron to a concrete mixture, the effectiveness of the concrete at shielding against neutrons should increase.

The second kind of material tested was polyethylene, a kind of plastic rich in hydrogen. 1 cm thick polyethylene sheets were cut into 10“ x 15“ sheets, large enough to block the entrance to the collimator. Polyethylene on its own should not be sufficient to block neutrons, but thanks to its hydrogenous nature they will transfer at least some of their energy to polyethylene. As such, they will have lower energy upon impacting other materials, meaning less of that material will be needed to provide the same level of shielding. Like with concrete, boron can also be added to polyethylene to increase its effectiveness at shielding against neutrons. 1” (2.54 cm) thick sheets of borated polyethylene were cut into sheets. The boron in the polyethylene should allow it to successfully block neutrons.

The final material tested was lead. 2” (5.08 cm) thick lead blocks were stacked on top of one another to create a wall. Lead is a poor material for shielding against neutrons (Martin, 2016, p. 660). However, it is one of the most effective materials at shielding against x-rays.

In addition to individual materials, combinations of materials were tested to see if any were more effective than the materials on their own. Two combinations were tested: polyethylene and borated polyethylene, and concrete and borated concrete. Originally, more combinations were intended to be tested, to verify which combination of materials were most effective. Unfortunately, with only two days' worth of experiments left to run, WPI's physical labs were closed due to the outbreak of COVID-19, and these experiments were not completed.

3.3 Procedure

Both the Remball and ion chamber have no method of remotely reporting their readings; readings must be made by a person with a direct line-of-sight to their display. However, it is unsafe for a human operator to remain in the room with the generator while it is operational, due to the relatively high absorbed dose they would receive. For the same reason, the lead-lined door to the room must remain closed, making it impossible to see the displays even from afar.

To get around this problem, before the generator accelerator was activated, a GoPro camera and a phone camera were activated to begin recording footage simultaneously. The GoPro would be attached to the Remball or ion chamber with a velcro strap, as illustrated in Figure 2.

Figure 2: The GoPro camera, attached to the handle of the remball with a velcro strap. The camera is aimed at the display of the remball, allowing its measurements to be recorded while the operator is outside of the room and unable to read it.

Then, the phone camera would be carried outside, and positioned so it had a line of sight to the computer screen that displayed the readouts of the various generator systems, including the accelerator current. The accelerator was then started and allowed to run for one minute. After this time, the GoPro would be retrieved, and both it and the phone camera would stop recording. These videos would later be analyzed to determine the absorbed dose rate in the collimator (a process which will be explained in-depth in section 3.4).

To determine the effectiveness of a given material at shielding for a specific kind of radiation, first a measurement was taken of the absorbed dose rate present in the empty collimator. Then, one “layer” of the material being studied (either one sheet of polyethylene or borated polyethylene, or a stack of concrete, borated concrete, or lead blocks) would be placed in the collimator, and a measurement taken. More layers would be added, and the process would be repeated.

3.4 Analysis

To analyze the data, the videos taken by the GoPro and phone camera for each run were played side-by-side, as shown in Figures 3A and 3B. After the generator had reached full power, at a given timestamp both videos were paused. For the remball, which has an analog display, these times were chosen to be moments when the needle pointer was directly over one of the tick marks as shown in Figure 3A, allowing for the maximum level of accuracy in each reading. For the ion chamber, which has a digital display, these times were chosen randomly. Then, the absorbed dose rate in mrem / hr, and the current through the accelerator, were both recorded. Because the current through the accelerator would often fluctuate several times in one second, a best guess was made as to which of the current readings was most accurate.

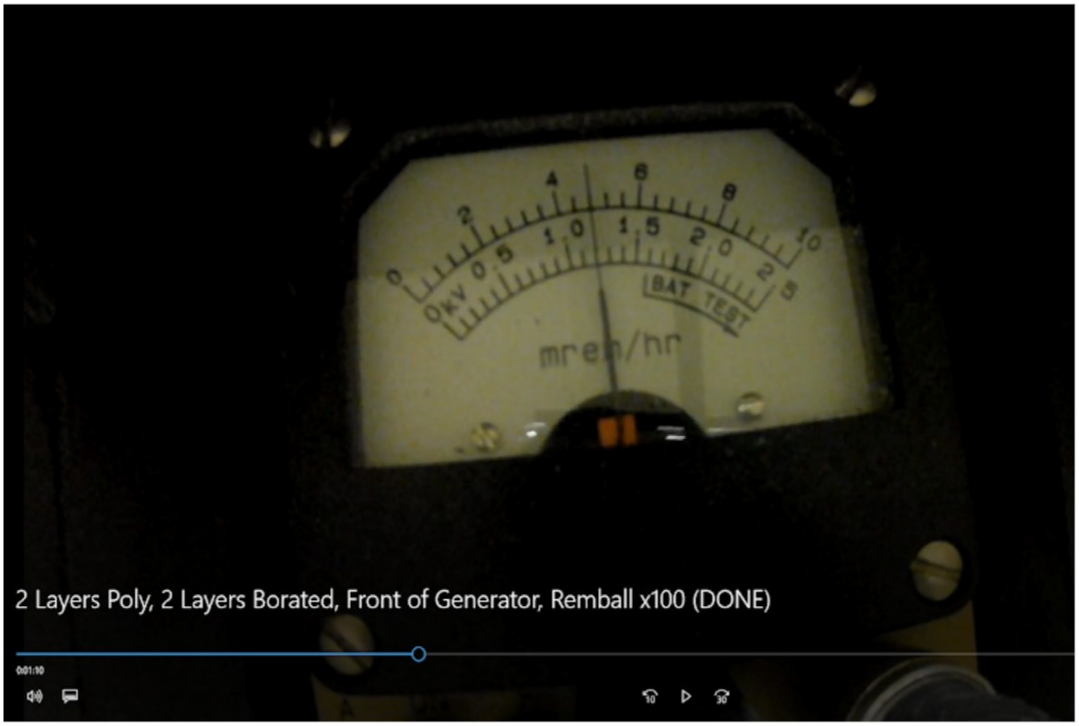

Figure 3A: The display of the remball, as it was recorded while there were two 1 cm thick layers of polyethylene and two 2.54 cm thick layers of borated polyethylene in the collimator in front of the generator. When the needled crossed over a tick mark (in this case, 480 mrem / hr), the video would be paused (in this case, at 1:10).

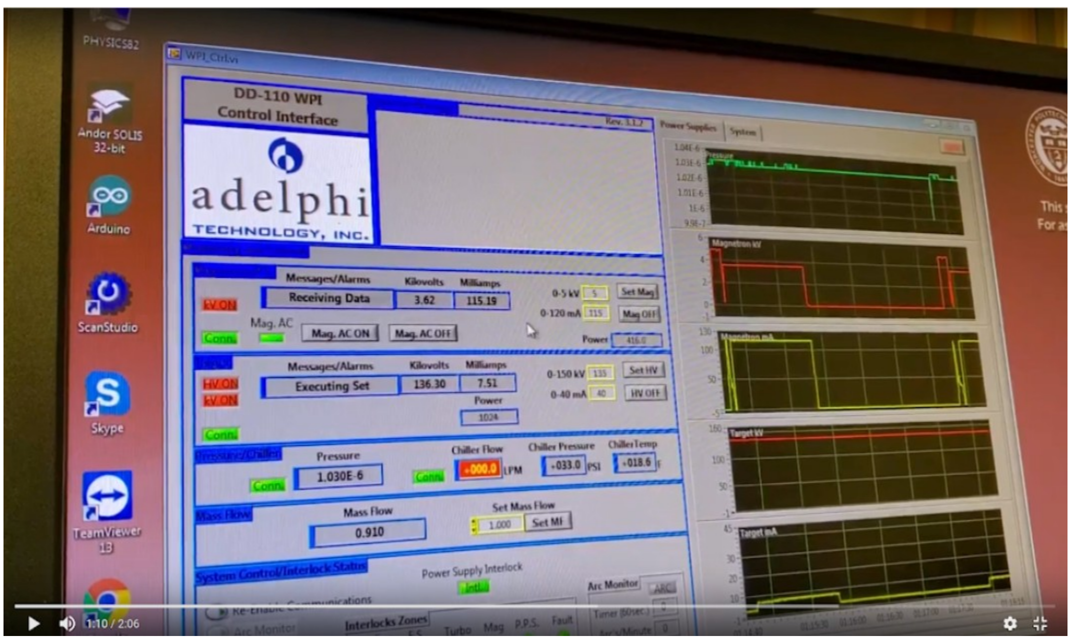

Figure 3B: The control panel of the neutron generator, as recorded by the phone camera while there was current through the plasma accelerator. The video was paused at 1:10, the same timestamp as the video of the remball was paused, so the current in the accelerator at that moment could be recorded.

The reason for recording accelerator current was to account for these fluctuations since current directly correlates to neutron fluence rate. Alinear relationship between the accelerator current and the dose rate was assumed -- as the current rose, the dose rate in the collimator would rise by the same proportion, and vice versa. Therefore, to prevent unintended changes in the current from skewing the data, the dose rate was normalized to the accelerator current. This was done by multiplying each dose rate measurement by a correction factor which was inversely proportional to the accelerator current. The exact formula I decided upon for the correction factor *f* was:

$$f = \frac{7.85\, mA}{I}$$

Where *I* is the accelerator current. The constant of 7.85 mA was chosen because it happened to be the accelerator current of the first data point that was analyzed. This meant that when the accelerator current increased above 7.85 mA, the correction factor would be less than 1, causing the corrected dose rate to decline. When it was greater, the correction factor would be greater than 1, causing the corrected dose rate to increase. Therefore, all dose rate measurements would be corrected to the level they "would" have been if the accelerator current was consistently 7.85 mA, removing a major source of error and allowing them to be compared with one another.

This process was repeated five times per experiment. Then, the five corrected dose rates were averaged, and their standard deviation was found. An example of a spreadsheet showing the observed dose rates, accelerator currents, correction factors, corrected dose rates, average, and standard deviation for one set of measurements is shown in Figure 4.

	A	B	C	D	E
1	2 Layers of Concrete (Day 2)				
2	First Run				
3	**Timestamp**	**Accelerator Curren (mA)**	**Dose Rate (mrem / hr)***	**Correction Factor**	**Corrected Dose Rate (mrem / hr; normalized to 1 mA)**
4	1:52	5.40	60	1.453703704	87.22222222
5	1:55	5.35	60	1.467289720	88.03738318
6	2:00	5.52	60	1.422101449	85.32608696
7	2:02	5.62	60	1.396797153	83.80782918
8	2:05	5.42	60	1.448339483	86.90036900
9				**Average:**	**86.25877811**
10				**Standard Deviation:**	**1.68673967**

Figure 4: A spreadsheet showing the five measurements collected for measurements of 2 layers of concrete, the timestamps at which they were recorded, the current through the accelerator at that time, and the correction factor and corrected dose rate calculated from this data.

Finally, the averages were graphed against the width of the material in the experiment. In keeping with shielding theory, an exponential best-fit line was used to model the stopping power equation. The coefficient of the exponent would be the mass attenuation coefficient. For determining the mass attenuation coefficient of a combination, this analysis was performed while keeping the width of one material was kept constant, while the width of the other was varied.

4. Results

4.1 Initial experimental design

The data taken for the dose rates due to thermal neutrons and gamma and x-rays in front of the generator had little deviation between each data point and the best-fit curves producing an exponentially decreasing neutron fluence rate as shielding thickness was increased. This exponential curve fits the theoretical shielding behavior of neutrons which are expected to have a transmission through material of $T = \exp(-\mu * x)$, as was discussed in section 2.3 of this report). An example is shown in Figure 5, which shows the observed dose rate due to thermal neutrons in concrete. A similar exponential curve is seen for all of the graphs of the dose rate measurements taken in front of the generator.

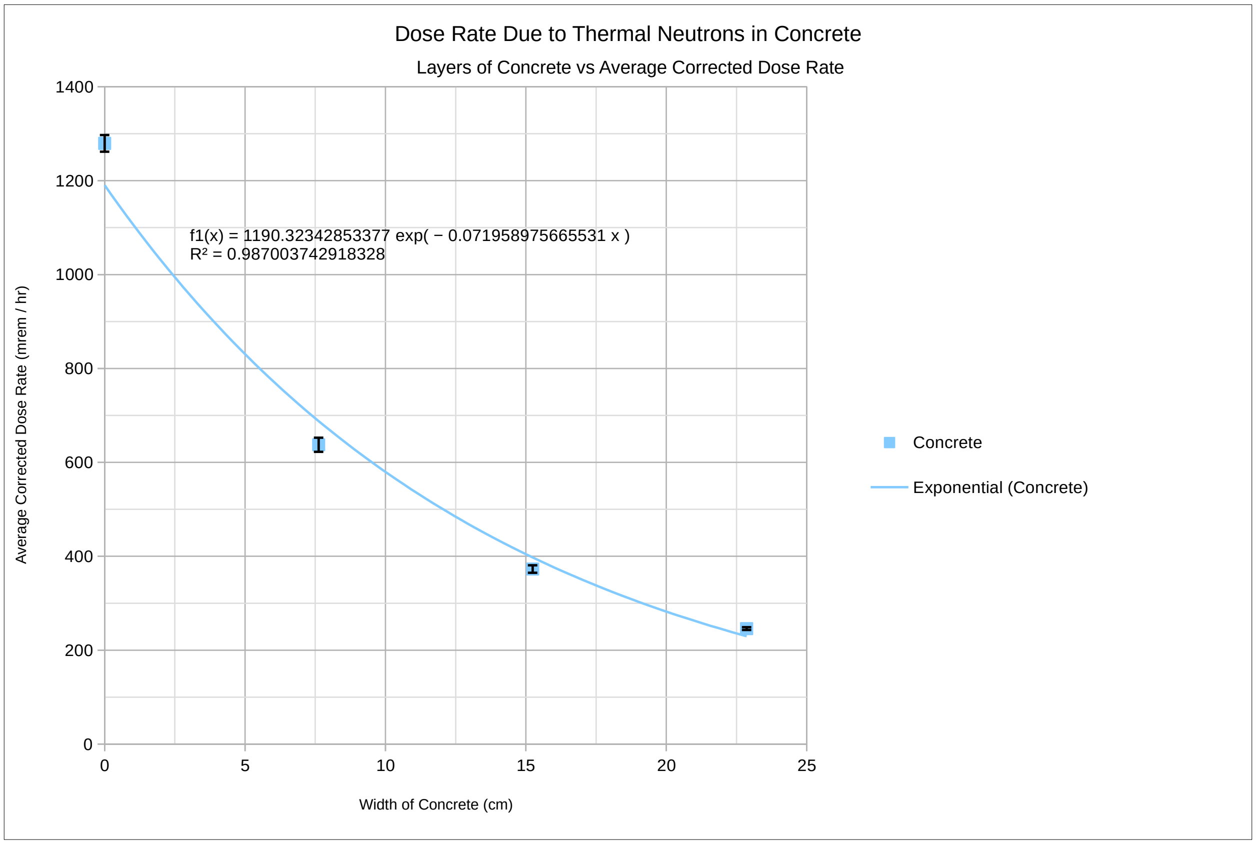

Figure 5: The average corrected dose rate present in the collimator versus the width of the concrete between it and the generator. Note the high coefficient of determination, indicating the data is almost perfectly in line with the theoretically predicted exponential curve. Also note the large absolute drop in the dose rate as the width of the concrete increases: there is nearly a 900 mrem / hr difference between the highest average corrected dose rate and the lowest.

However, this was not the case for the data taken for fast neutrons and gamma and x-rays at the side of the generator. Most graphs showed very little difference in the dose rate no matter the width of the material being studied. This is illustrated by Figure 6, which shows the observed dose rate due to fast neutrons in concrete.

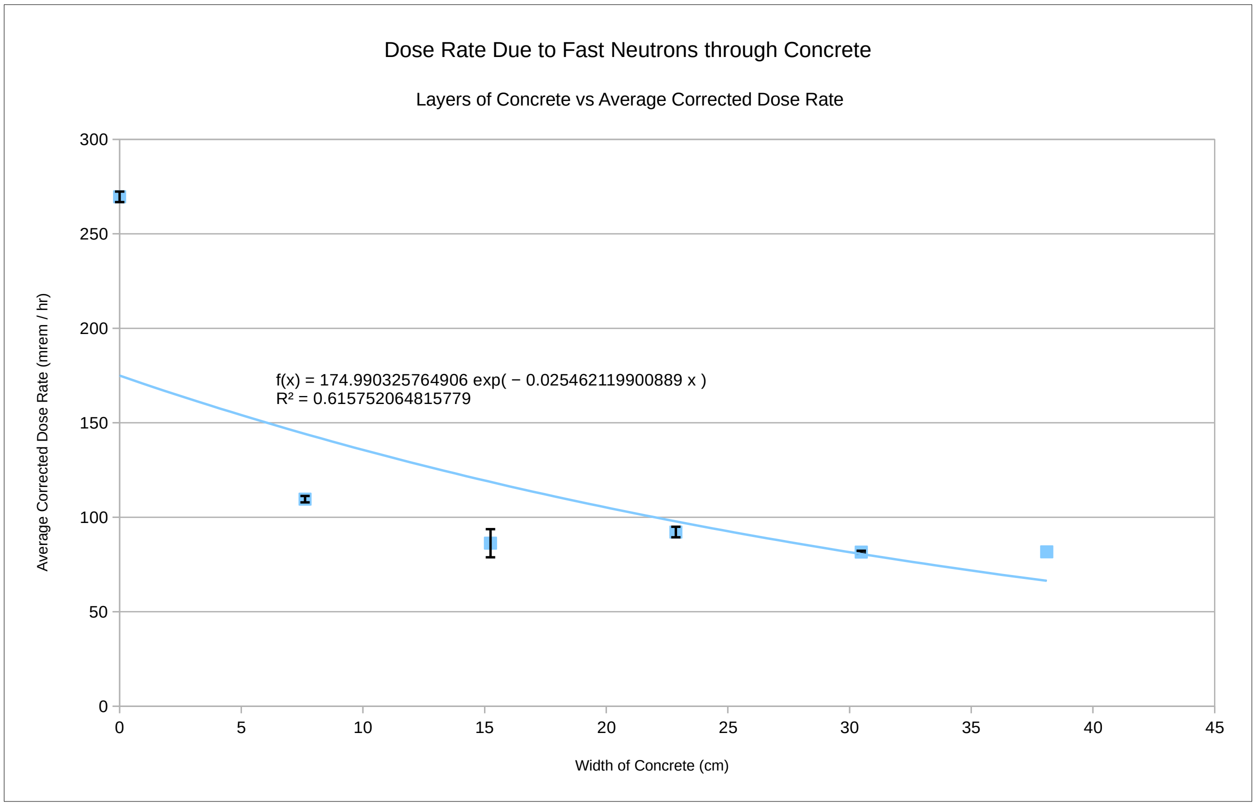

Figure 6: The average corrected dose rate present in the collimator versus the width of the concrete between it and the generator. Note the low coefficient of determination, indicating the data does not align with the theoretically predicted exponential curve, and the small difference between the highest and lowest recorded dose rates.

This large variance, in combination with the relatively low difference between the absorbed doses measured even as the width of the material being studied was increased, suggests that there was a high level of background radiation present when the measurements were taken. The most likely explanation for this effect was a flaw in the design of the collimator built at the side of the generator. Investigation soon revealed that this was, indeed, the case: I had neglected to provide any kind of shielding to the base of the collimator. This meant that radioactive particles could bounce off the concrete floor of the lab, travel through the thin aluminum table on which the collimator rested and enter the Remball or ion chamber unimpeded. (here, the base of the collimator built in front of the generator was not initially shielded, but because the table on which it rested happened to have a surface made of 2.54 cm thick borated polyethylene, it functioned as a shielded base on its own.)

My original intention was to rectify the design of the collimator and perform the experiments for measuring shielding properties for fast neutrons once again. However, before I could do so WPI's physical labs were closed due to the outbreak of COVID-19, and these experiments were not completed.

4.2 Materials

There were no major issues in conducting any of the experiments on any of the individual materials. Aside from the aforementioned trouble with the collimator at the side of the generator, the only major event that did not go to plan was the arrival of the SARS-CoV-2 virus in Massachusetts. The COVID-19 outbreak forced the closure of the lab before the final experiments could be completed. These would have included reconducting the tests of materials' effectiveness at shielding against fast neutrons with a functioning collimator and testing the two or three most promising combinations of materials based on the data collected up until that point.

4.3 Analysis

The graphs of the absorbed dose rate of various kinds of radiation in the various materials tested are shown in Appendix A. From these graphs, the mass attenuation coefficients for fast neutrons, thermal neutrons, and gamma and x-rays were found. These results are shown in the tables below. (Note that only one material, concrete, had enough valid data from the experiments with fast neutrons to find a mass attenuation coefficient. Additionally, some mass attenuation coefficients were found from graphs with an R^2 value of 1.000. This is because these graphs had only two data points, allowing a perfect fit to the exponential curve even though the validity of the curve is in question due to the lack of data.)

Table 1: Mass Attenuation Coefficient for Gamma Rays and X-Rays

Material	**Mass Attenuation Coefficient (cm^2/g)**	**Coefficient of Determination / R^2**
Lead	0.104	0.991

Table 2: Mass Attenuation Coefficient for Thermal Neutrons, Single Materials

Material	**Mass Attenuation Coefficient (cm^2/g)**	**Coefficient of Determination / R^2**
Concrete	0.0720	0.987
Polyethylene	0.0174	1.000
Borated Polyethylene	0.167	1.000

Table 3: Mass Attenuation Coefficient for Fast Neutrons, Single Materials

Material	**Mass Attenuation Coefficient (cm^2/g)**	**Coefficient of Determination / R^2**
Concrete	0.0255	0.616

In addition to these single materials, the combined mass attenuation coefficient of the combinations I tested -- normal concrete and borated concrete, and polyethylene and borated polyethylene -- for thermal neutrons are shown in Table 4.

Table 4: Mass Attenuation Coefficient for Thermal Neutrons, Combinations of Materials

Material	**Mass Attenuation Coefficient (cm^2/g)**	**Coefficient of Variance / R^2**
Concrete, with 2.54 cm Borated Concrete	0.0716	0.997
Polyethylene, with 2.54 cm Borated Polyethylene	0.0616	1.000
Polyethylene, with 5.08 cm Borated Polyethylene	0.0861	0.997
Borated Polyethylene, with 2 cm Polyethylene	0.183	0.949
Borated Polyethylene, with 4 cm Polyethylene	0.181	1.000
Borated Polyethylene, with 6 cm Polyethylene	0.197	0.949
Borated Polyethylene, with 8 cm Polyethylene	0.199	1.000

As Table 4 shows, there is little difference in the mass attenuation coefficient for borated polyethylene no matter how many layers of polyethylene are placed in front of it -- as the presence of the polyethylene shouldn't change the properties of the borated polyethylene itself. However, when looking at a graph of the average dose rate in the collimator versus the width of borated polyethylene, it becomes clear that as the amount of polyethylene is increased, the average dose rate present at a given width of borated polyethylene decreases. This is illustrated in Figure 7.

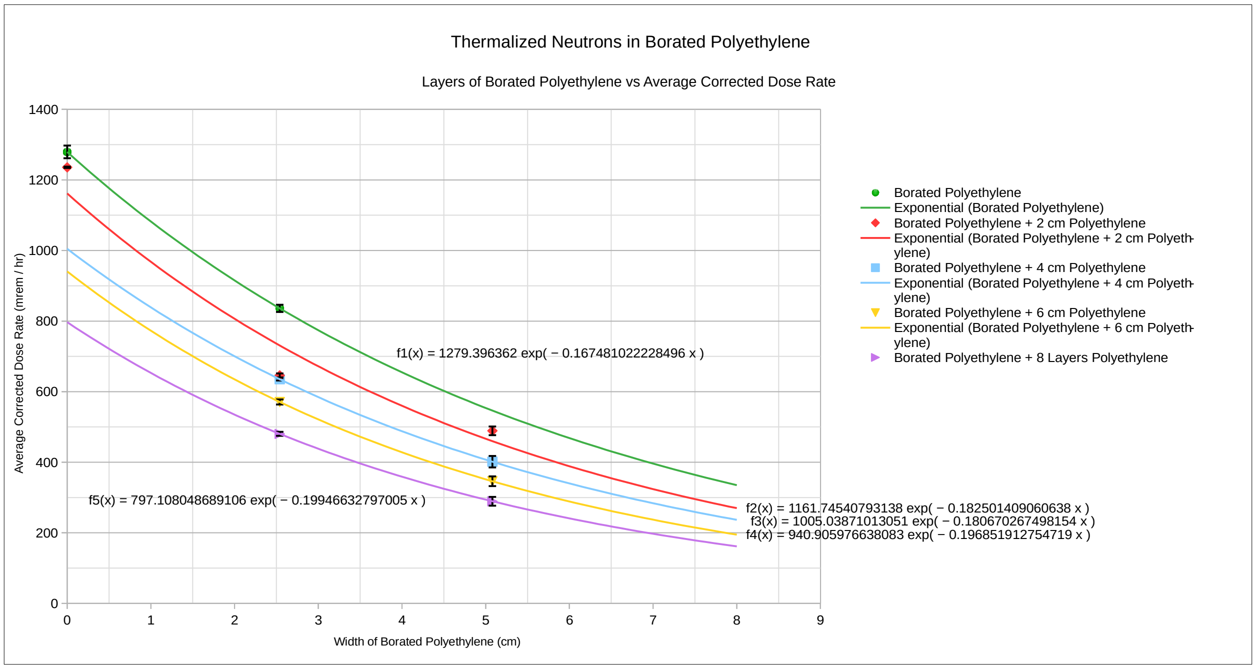

Figure 7: A graph of the average dose rate in the collimator versus the width of borated polyethylene. The black error bars represent the standard of deviation of each average corrected dose rate measured in the collimator for a given width of polyethylene. The coefficients of variation for each trendline have been omitted for ease of legibility.

This suggests that the presence of the polyethylene increases the effectiveness of the borated polyethylene at shielding against thermal neutrons. The same effect can be observed for the combination of borated concrete and non-borated concrete.

5. Discussion

The results for the effectiveness of shielding against x-rays and gamma rays clearly indicate that lead is the most effective material -- no surprise, as it was the only material tested for this purpose. For thermal neutrons, it is similarly clear the most effective material is clearly borated polyethylene but using it in combination with polyethylene decreases the total absorbed dose that will successfully penetrate the shielding. Therefore, for shielding against these two kinds of radiation, a system consisting of a combination of polyethylene, borated polyethylene, and lead will be most effective at shielding. Unfortunately, similar results could not be determined for my fast neutron experiments due to the poor quality of the data.

6. Conclusions

The findings of my research partially confirmed my hypothesis. As expected, lead was extremely effective at shielding against x-rays and gamma rays. However, concrete proved to be the worst material of any studied at shielding against thermal neutrons, while borated concrete fared little better. Rather, a combination of polyethylene and borated polyethylene proved most effective.

6.1 Future work

The most logical future work to be done is the work I would have done if the school hadn’t shut down: conducting the experiments to determine the efficacy of materials at shielding against fast neutrons once again, this time with a functioning collimator. Once this task is completed, the next step would be testing the precise combination of polyethylene, borated polyethylene, lead, and whichever material proves most effective at shielding against fast neutrons, in order to determine what combination of the materials would form the most effective shielding system for the three kinds of radiation produced by the generator.

Future researchers could also expand upon my work by studying the properties of other materials I did not have access to for potential use in a shielding system. Additionally, they could take into account other constraints in selecting a shielding system. For example, the generator is designed to be somewhat portable: it is relatively small in size and mounted on wheels, so it can be easily moved into and around a laboratory. Therefore, researchers might attempt to design a shielding system that keeps the mass of the generator as low as possible without sacrificing safety. Another potential factor that researchers might take into account is cost: the cheaper the shielding system, the cheaper the generator, meaning that more labs would be able to afford one and more research could be done.

Appendix A

Graphs of the Average Absorbed Dose Rate In Tested Materials

The following graphs show the average absorbed dose rate in the various materials tested over the course of this project due to the three main kinds of radiation produced by the generator. Each data point represents the average corrected dose rate in the collimator when a certain width of material is present between the remball or ion chamber and the generator. The black error bars represent the standard deviation of this average; note that in many cases, the standard of deviation is quite small compared to the measured values, so these bars may be hard to see. Finally, each set of measurements has an exponential best fit line associated with it, whose exponential coefficient represents the mass attenuation coefficient of the material. The coefficient of determination, or R^2 value, represents how accurately the equation fits the data points, with a value of 1 representing a perfect fit. However, while some of these equations do indeed have an R^2 value of 1.000, this is because these graphs had only two data points, allowing a perfect fit to the exponential curve even though the validity of the curve is in question due to the lack of data.

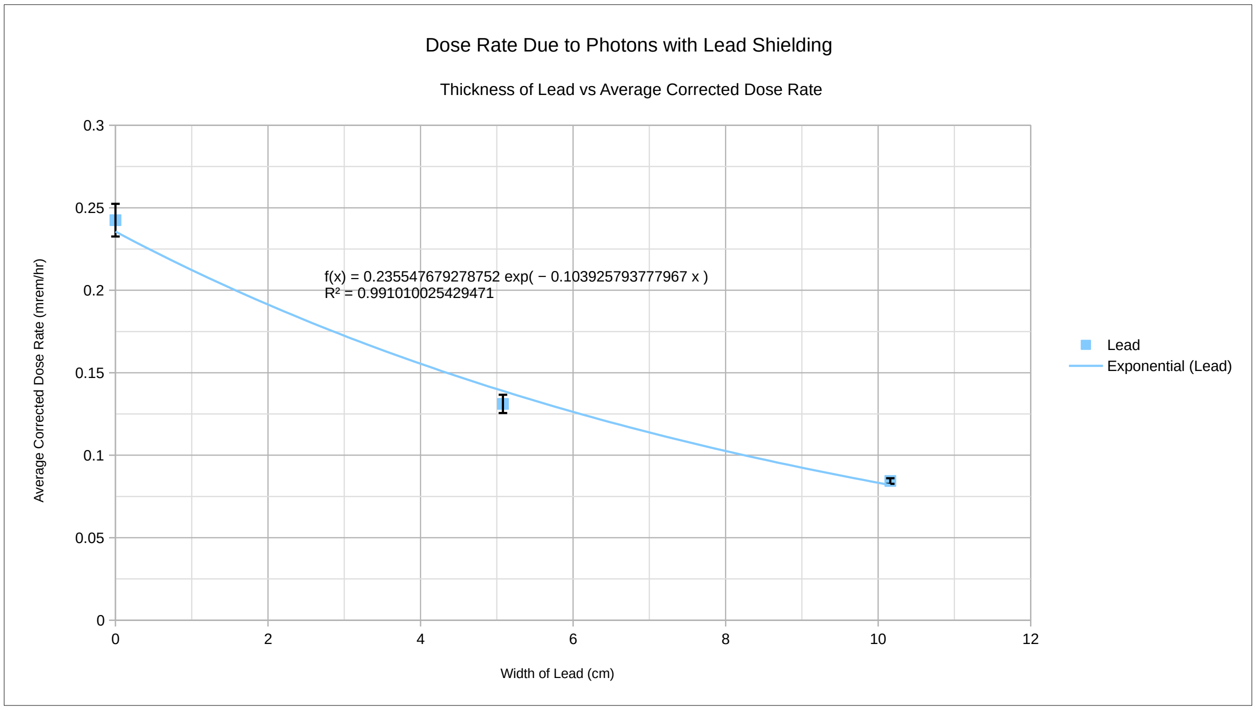

Figure 8: A graph of the average dose rate in the collimator due to photon radiation versus the width of lead.

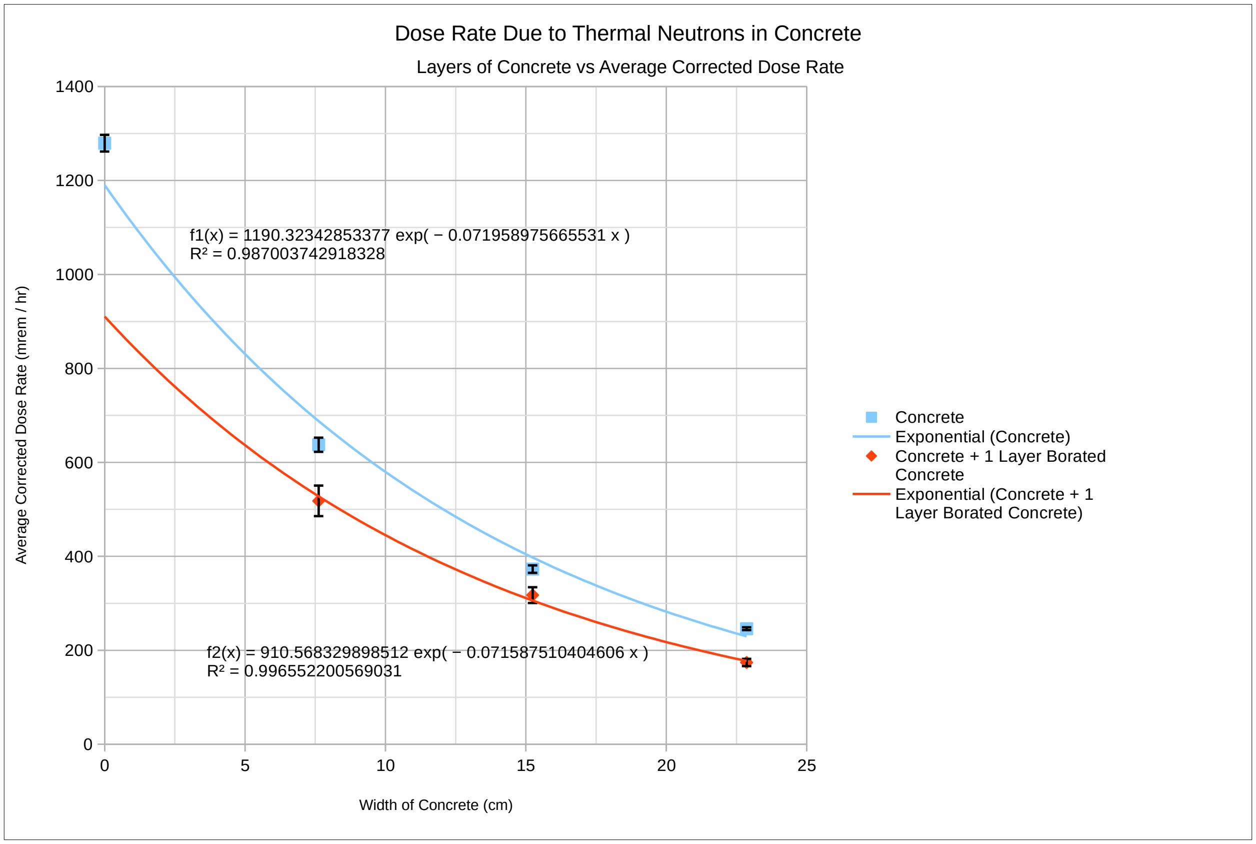

Figure 9: A graph of the average dose rate in the collimator due to thermal neutrons versus the width of concrete.

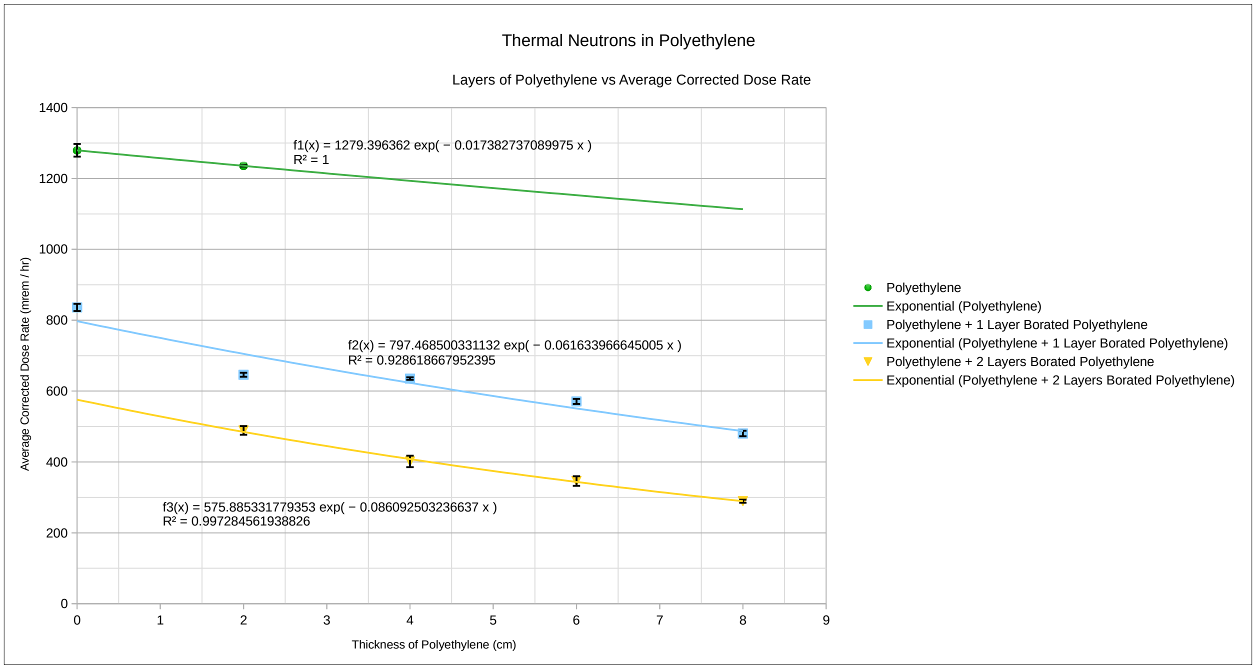

Figure 10: A graph of the average dose rate in the collimator due to thermal neutrons versus the width of polyethylene.

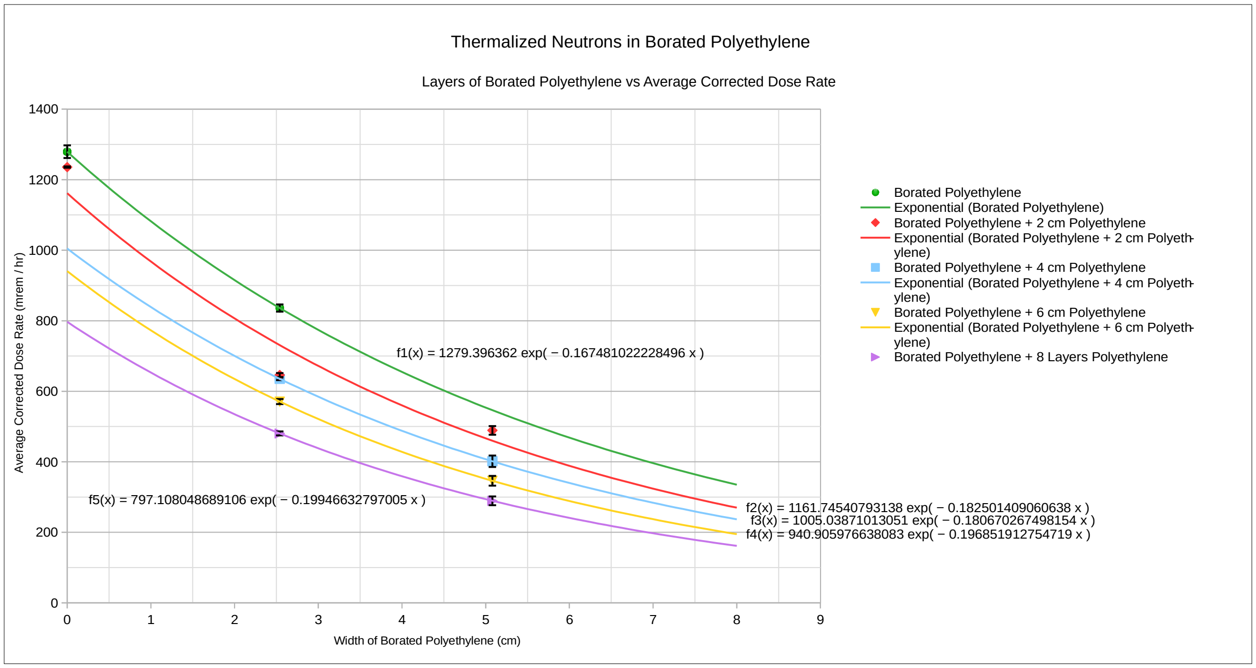

Figure 11: A graph of the average dose rate in the collimator versus the width of borated polyethylene. The coefficients of variation for each trendline have been omitted for ease of legibility; they can be found in Table 4 in section 4.3.

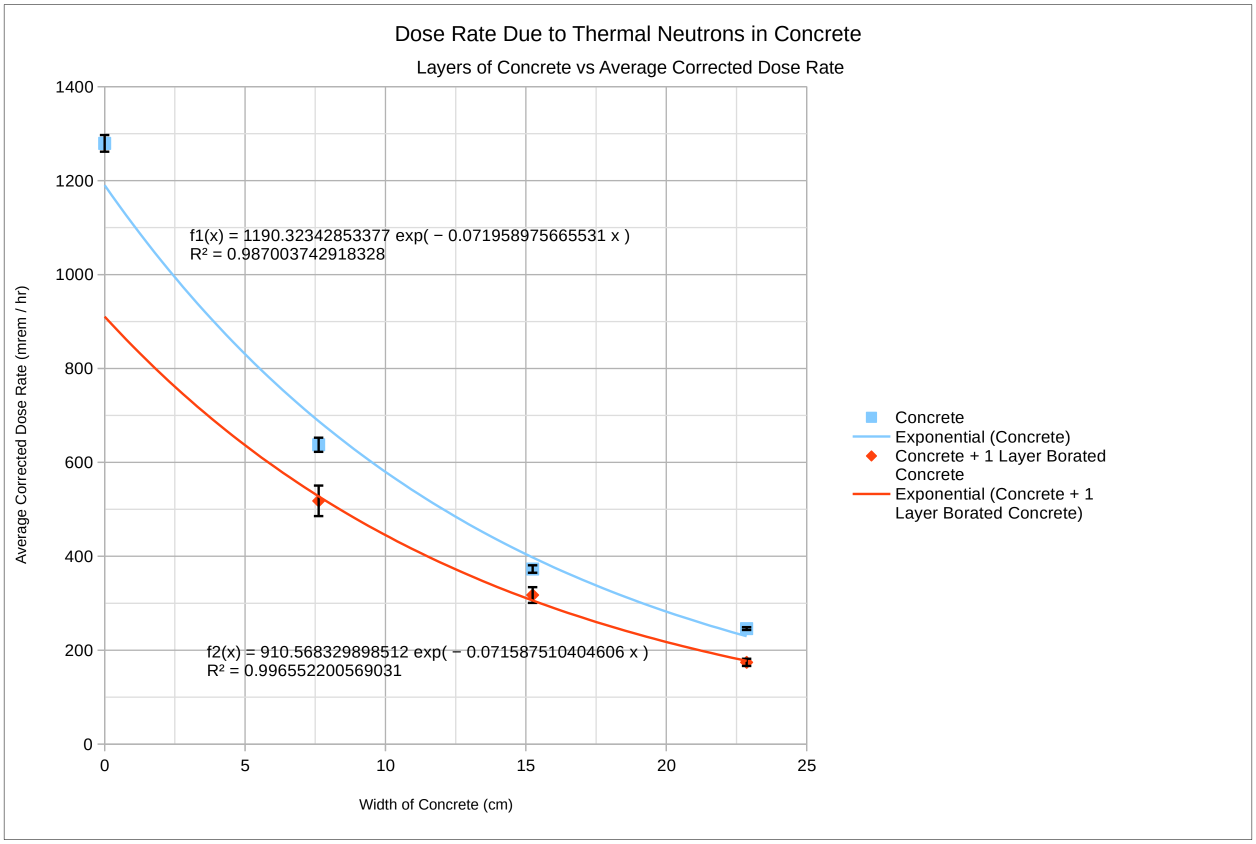

Figure 12: The average corrected dose rate present in the collimator versus the width of the concrete between it and the generator. Note the low coefficient of determination, indicating the data does not align with the theoretically predicted exponential curve, and the small difference between the highest and lowest recorded dose rates.

References

Adelphi Technology, Inc. (2016, May 27). *Neutron Generator Models DD-109M & DD110M Operation Manual.*

Chichester, D. L., & Blackburn, B. W. (2007). Radiation Fields from Neutron Generators Shielded with Different Materials. *Nuclear Instruments and Methods in Physics Research Section B: Beam Interactions with Materials and Atoms*, *261*(1-2), 845–849. doi:10.1016/j.nimb.2007.04.222

Editors of Encyclopaedia Brittanica. (2018, November 95). Thermal Neutron. Retrieved from https://www.britannica.com/science/thermal-neutron

Kunashenko, Y. P. (2011, September 16). Coherent Bremsstrahlung from Fast Neutrons. Retrieved from https://indico.cern.ch/event/153576/contributions/1397948/attachments/161797/228345 Kunashenko_Tuesday.pdf

Lou, T. P. (2003). *Compact D-D/D-T Neutron Generators and Their Applications* [Doctoral dissertation, University of California, Berkeley].

Martin, J. (2013). *Physics for Radiation Protection* (3rd ed.). Ann Arbor, MI: Wiley-VCH.